nucleon rather than by the total number of states available, we might expect to observe a relatively small cross section for the $Al^{27}(\gamma,\pi^+)Mg^{27}$ reaction. A quantitative prediction would require information about both the number of final states available for population in Mg^{27} and the number of initial protons available for the pion production process. Such a prediction can not be made until more detailed information about the nature of the level structure in Mg^{27} is available. However, it does appear that this type of extension of the Laing-and-Moorhouse theory could account for our results.

ACKNOWLEDGMENTS

We would like to acknowledge the contribution made by the operating and engineering staff of the 300-MeV betatron facility in making the irradiations possible. We would also like to acknowledge the assistance of K. Borden, E. Diefallah, W. Switzer, and J. Drake in performing some of the experiments and helping with the reduction of data. One of us (WBW) held a National Science Foundation predoctoral fellowship during part of the time that this work was in progress.

PHYSICAL REVIEW VOLUME 143, NUMBER 3 MARCH 1966

Study of Nucleon-Nucleus Elastic Scattering in Second-Order Multiple-Scattering Theory*

F. A. McDonald† and M. H. Hull, Jr.
Yale University, New Haven, Connecticut
(Received 4 October 1965)

Nucleon-nucleus scattering is studied in the energy range 95–350 MeV for targets ranging from carbon to lead. The relative importance of the first and second order terms in Watson's multiple-scattering expansion of the optical potential in terms of the two-nucleon scattering matrix is investigated with the nucleon-nucleon phase parameters obtained at Yale. Effects of including the angular dependence of the two-nucleon amplitudes, as Cromer has done, are compared with those of the second-order potential, and they are found to be equally important so that both must be included for consistency. The possibility of investigating nuclear-structure parameters, especially the two-nucleon correlation lengths brought in by the second-order potential, is considered.

I. INTRODUCTION

THE treatment of inelastic processes which remove the incident nucleon from the entrance channel in nucleon-nucleus scattering by including an imaginary part in the potential representing the interaction was introduced by Ostrofsky, Breit, and Johnson.[1] The method was further investigated by Bethe,[2] and several early analyses[3] demonstrated the ability of the optical model to correlate scattering data over a range of energies and targets with relatively few parameters. Continued successes with this model have inspired extensive phenomenological analyses, with many refinements of detail receiving careful attention. The review in Hodgson's book[4] summarizes much of this work.

The assumed potential has the form

$$V(r)=(U_c+iW_c)\rho(r)+\left(\frac{\hbar}{\mu c}\right)^2(U_s+iW_s)\frac{1}{r}\frac{d\rho}{dr}(\boldsymbol{\sigma}\cdot\mathbf{L}), \quad (1)$$

where the potential strengths are adjustable parameters, and $\rho(r)$ is a dimensionless radial function that is nearly constant from $r=0$ to the nuclear radius and there falls rapidly but smoothly to very small values. It is natural to assume that $\rho(r)$ has some connection with the distribution of matter in the nucleus, so that the range R_h (defined as the distance at which $\rho(r)$ has half its maximum value) will depend on $A^{1/3}$, where A is the mass number. However, both range and surface thickness, t_s (the distance in which the radial function falls from 90% to 10% of its central value) are treated as adjustable. The electron-scattering experiments, analyzed in terms of a similar $\rho(r)$,[5] show a discrepancy when compared with the results of nucleon-nucleus scattering experiments: the extent of the nuclear-matter distribution is smaller for electron scattering than for nucleon scattering. More sophisticated phenomenological analyses by Hodgson[6] show that a satisfactory

* This research was supported by the U. S. Atomic Energy Commission and by the U. S. Army Research Office-Durham.
† Now at Texas A. & M. University, College Station, Texas.
[1] M. Ostrofsky, G. Breit, and D. P. Johnson, Phys. Rev. **49**, 22 (1936).
[2] H. A. Bethe, Phys. Rev. **57**, 1125 (1940).
[3] S. Fernbach, R. Serber, and T. B. Taylor, Phys. Rev. **75**, 1352 (1949); R. E. LeLevier and D. S. Saxon, Phys. Rev. **87**, 40 (1952); H. Feshbach, C. E. Porter, and V. F. Weisskopf, Phys. Rev. **96**, 448 (1954).
[4] P. E. Hodgson, *The Optical Model of Elastic Scattering* (Oxford University Press, London, 1963).
[5] R. Hofstadter, Ann. Rev. Nucl. Sci. **7**, 231 (1957).
[6] P. E. Hodgson, Phys. Rev. Letters **6**, 358 (1961).

fit to diffraction minima in nucleon-nucleus scattering angular distributions requires that the range of the real and imaginary potentials in Eq. (1) be different, with the imaginary part having a somewhat longer range.

The success of the optical model in correlating so wide a range of experiments has led to various attempts at its theoretical justification. The complexities of the many-body problem are severe, and initial attempts have been based on Chew's[7] impulse approximation: the energy of the incident nucleon is assumed to be high enough so that the target can be considered to be a collection of independent nucleons. Watson's[8] multiple-scattering analysis has employed this approximation, and he has shown how, with suitable approximations, an effective nucleon-nucleus potential of the form of Eq. (1) can be obtained, with the strength parameters directly related in first order to the nucleon-nucleon scattering matrix. Köhler[9] and Levintov[9] have shown that for a potential in which the radial dependence of the central and spin-orbit parts are related as in Eq. (1), the small-angle polarization is correctly given in first Born approximation. This experimental quantity is therefore directly related, via the impulse approximation, to the nucleon-nucleon scattering matrix, as Bethe[10] has emphasized. Consistency between nucleon-nucleon and nucleon-nucleus scattering through such a polarization calculation has been demonstrated by Ohnuma,[11] Bethe,[10] and Wilson[12] and general agreement with the cross section was obtained by Riesenfeld and Watson.[13]

Watson's treatment leads to an expansion of the effective potential, in which the leading term involves a sum of two-nucleon scattering amplitudes over the target nucleons. It is therefore straightforward to compare calculated strength functions, in this approximation, with phenomenological parameters such as collected by Hodgson.[4] Several authors have done so[14] and demonstrated reasonable consistency. The phenomenological parameters are hardly unique, however.[4] The next term in Watson's expansion includes effects of scattering to an intermediate inelastic state, followed by return to ground. This will be called the second-order potential, and it has been obtained by Johnston and Watson[15] in an approximation allowing practical calculations. The usual first-order potential calculations have employed only the forward angle values of the nucleon-nucleon scattering matrix, and Cromer[16] has investigated effects of taking into account the angular variations of the amplitudes. In the present work, these effects have been found to be comparable with those of the second-order potential, though different in character, so that a consistent treatment should employ them both.

The present calculation of the optical potential still employs three major approximations: (1) the impulse approximation itself, which ignores effects of binding of the target nucleons to one another; (2) target nucleon momentum is neglected; (3) the nucleon-nucleon scattering matrix used is that derived from analyses of elastic two-nucleon scattering, so that it depends only on momentum transfer and any effects of "off-energy-shell" matrix elements are lost. The phenomenological results of nucleon-nucleon scattering analyses obtained by Breit *et al.*[17] and Hull *et al.*[18] are used, and some comparisons of effects of using other representations[19] of the two-nucleon scattering matrix are made, including recent improvements in the many-energy analyses.[20] Angular distributions in scattering and polarization, given by employing the potentials obtained in a Schrödinger equation, are compared with data in the energy range 84–350 MeV for the incident nucleon and for targets ranging from carbon to lead. Estimates of the importance of the remaining approximations are made, and the possibility of determining the nuclear structure parameters specifying nucleon distribution and correlations is examined.

II. EVALUATION OF THE POTENTIAL

The problem to be solved formally is that of finding a potential, $V_{\rm op}$ such that the single-particle Schrödinger equation

$$(h+V_{\rm op})\lambda_k'=\epsilon_0\lambda_k' \tag{2}$$

represents the nucleon-nucleus scattering. Here h is the nucleon kinetic energy operator, ϵ_0 the nucleon energy in the nucleon-nucleus center-of-mass system (Nc.m. system). Johnston and Watson[15] have shown that a formal solution of the problem is provided by the multiple-scattering expansion

$$V_{\rm op}=\sum_{\alpha=1}^{A}\langle t_\alpha\rangle+\sum_{\alpha,\beta\neq\alpha}\left\langle t_\alpha\frac{1}{a}P_{ND}t_\beta\right\rangle + \sum_{\alpha,\beta\neq\alpha,\gamma\neq\beta}\left\langle t_\alpha\frac{1}{a}P_{ND}t_\beta\frac{1}{a}P_{ND}t_\gamma\right\rangle+\cdots. \tag{3}$$

[7] G. F. Chew, Phys. Rev. **80**, 196 (1956); G. F. Chew and G. C. Wick, Phys. Rev. **85**, 636 (1952); G. F. Chew and M. L. Goldberger, Phys. **87**, 778 (1952).
[8] K. M. Watson, Phys. Rev. **89**, 575 (1953); N. C. Francis and K. M. Watson, Phys. Rev. **92**, 291 (1953).
[9] H. S. Kohler, Nucl. Phys. **1**, 433 (1956); I. I. Levintov, Doklady Akad. Nauk. SSSR **107**, 240 (1956) [English transl.: Soviet Phys.—Doklady **1**, 175 (1956)].
[10] H. A. Bethe, Ann. Phys. (N. Y.) **3**, 190 (1958).
[11] S. Ohnuma, Phys. Rev. **111**, 1172 (1956).
[12] R. Wilson, Phys. Rev. **114**, 260 (1959).
[13] W. B. Riesenfeld and K. M. Watson, Phys. Rev. **102**, 1157 (1956).
[14] References 10, 12, 13 and A. K. Kerman, H. McManus, and R. M. Thaler, Ann. Phys. (N. Y.) **8**, 551 (1958); A. H. Cromer, Phys. Rev. **113**, 1607 (1959); A. Johansson, U. Swanberg, and R. E. Hodgson, Arkiv Fysik **19**, 541 (1961); J. Dabrowski and J. Sawicki, Nucl. Phys. **13**, 621 (1959); **22**, 318 (1961); J. Dabrowski and A. Sobiczewski, Nuovo Cimento **20**, 403 (1961), and Acta Phys. Polon. **20**, 243 (1961).
[15] R. R. Johnston and K. M. Watson, Nucl. Phys. **28**, 583 (1961); R. R. Johnston, *ibid.* **36**, 368 (1962).
[16] A. H. Cromer, Phys. Rev. **113**, 1607 (1959).
[17] G. Breit, M. H. Hull, Jr., K. Lassila, and K. D. Pyatt, Phys. Rev. **120**, 2227 (1960); *ibid.* **128**, 826 (1962).
[18] M. H. Hull, Jr., K. E. Lassila, H. M. Ruppel, F. A. McDonald, and G. Breit, Phys. Rev. **122**, 1606 (1961); **128**, 830 (1962).
[19] J. Gammel and R. M. Thaler, Phys. Rev. **107**, 291, 1337 (1957).
[20] G. Breit, A. N. Christakis, M. H. Hull, Jr., H. M. Ruppel, and R. E. Seamon, Bull. Am. Phys. Soc. **9**, 378 (1964).

It has been assumed that the incident nucleon interacts with nuclear particles via two-body potentials v_α, and thus t_α is a two-body scattering operator defined by

$$t_\alpha = v_\alpha + v_\alpha \frac{1}{a} t_\alpha, \tag{4}$$

where the propagator a, appearing also in Eq. (3), is

$$a = E_\alpha - H_0 + i\eta. \tag{5}$$

Here E_α is the sum of ϵ_0 and the nuclear ground-state energy, H_0 the sum of nucleus and nucleon Hamiltonians in the absence of incident nucleon-nucleus interactions, and η determines the boundary conditions in the usual way.[21] In Eq. (3) the brackets denote evaluation of relevant matrix elements for the nuclear ground state, and P_{ND} is a projection operator which is zero when acting on the ground state and unity otherwise. The subscript ND signifies "nondiagonal" in the notation of Watson.[8,15] It should be noted that antisymmetrization has only been approximately taken into account; the nuclear wave functions are antisymmetrized, as are the two-nucleon scattering matrices, but the complete antisymmetrization of $(A+1)$ nucleons has not been carried out. Takeda and Watson[22] have shown that this neglects "target exchange" effects, wherein a nuclear particle other than the αth nucleon exits with the high energy of the incident nucleon, leaving the incident nucleon in the nucleus.

Other expansions of $V_{\rm op}$ are possible. Among them are those of Kerman *et al.*[23] (hereafter denoted by KMT) and of Francis and Watson.[24] The differences may be summarized by saying that different propagators are chosen, requiring therefore solutions of different two-body problems. In the KMT calculations, the first-order term is the same as in Eq. (3), but the second-order term contains contributions of the third order in the Johnston-Watson expansion, which has elastic scattering in intermediate states. For the Francis-Watson expansion, the two-body scattering operator is defined with a propagator in which the projectile energy is corrected to that in the nuclear medium. This implies a self-consistent calculation, since the modified energy depends on the two-body scattering matrix. It has not been determined in the present study which of these expansions converges best. The Johnston-Watson expansion recommends itself as straightforward in applications, and some estimates of corrections to it are attempted.

The potential of Eq. (3) is nonlocal and formally requires solution of the full many-body problem, because the propagator $(1/a)$ contains the nuclear Hamiltonian; for the same reason, $\mathbf{t}_\alpha$ is not the free two-body scattering operator. However, use of the impulse approximation implies neglect of the binding of the αth particle to its neighbors in the nucleus, so that $\mathbf{t}_\alpha$ may be replaced by the free-scattering operator, t_α. For the projectile energies considered, one may also neglect initial target-nucleon momenta compared to the incident-nucleon momentum, and hence t_α acts on the nuclear ground state only through the spin and isospin coordinates. A local potential results from the assumption that the matrix element of t_α depends on the final state of the scattered nucleon only through $\mathbf{q}$, the momentum transfer; this neglects "off-energy-shell" effects in t, which arise because the projectile is actually scattering off a heavy nucleus in the Nc.m. system (kinematic differences in t *are* included).

The first-order term in the potential, in coordinate space, is then

$$\langle \mathbf{r}' | V^{(1)} | \mathbf{r} \rangle \equiv \delta(\mathbf{r}'-\mathbf{r}) V^{(1)}(\mathbf{r}) = \delta(\mathbf{r}'-\mathbf{r}) A \int d^3q\, F(q) \bar{t}(q) \exp(i\mathbf{q}\cdot\mathbf{r}), \tag{6}$$

where A is the nuclear mass number, $F(q)$ is the Fourier transform of the nuclear density function $\rho(r)$, and $\bar{t}(q)$ is the spin-isospin average over target nucleons. The nucleon-nucleon scattering matrix may be written in spin space as[25]

$$M(\theta_c) = A(\theta_c) + C(\theta_c)(\boldsymbol{\sigma}_1+\boldsymbol{\sigma}_2)\cdot\mathbf{n} + B(\theta_c)(\boldsymbol{\sigma}_1\cdot\mathbf{n}\boldsymbol{\sigma}_2\cdot\mathbf{n}) + \tfrac{1}{2}G(\theta_c)(\boldsymbol{\sigma}_1\cdot\mathbf{m}\boldsymbol{\sigma}_2\cdot\mathbf{m} + \boldsymbol{\sigma}_1\cdot\mathbf{l}_2\boldsymbol{\sigma}\cdot\mathbf{l}) + \tfrac{1}{2}H(\theta_c)(\boldsymbol{\sigma}_1\cdot\mathbf{m}\boldsymbol{\sigma}_2\cdot\mathbf{m} - \boldsymbol{\sigma}_1\cdot\mathbf{l}\boldsymbol{\sigma}_2\cdot\mathbf{l}), \tag{7}$$

where θ_c is the scattering angle in the two-nucleon zero-momentum system (the c.m. system), $\boldsymbol{\sigma}_i$ the spin operators for the two nucleons, $\mathbf{n}$ a unit vector normal to the scattering plane which forms, with $\mathbf{m}$ and $\mathbf{l}$, a right-handed coordinate system. The first-order spin averages leave only $A(\theta_c)$ and $C(\theta_c)$ contributing to the optical potential.

The second-order term requires more strenuous effort for its evaluation in the Johnston-Watson treatment,[15] and the following approximations or assumptions are made. Energy differences between excited and ground states are ignored compared to ϵ_0 so that closure may be used in the reduction of the sum on α, β. Not only is $\mathbf{t}_\alpha$ replaced by t_α on the two-nucleon energy shell, but only t_α^0, the value at forward angles, is employed. This last replacement is consistent with the assumption that the second-order contribution will be smaller than the first, so the refinement of taking the angular variation of t_α into account is unnecessary for the second order. In fact numerical evaluation confirms that it *is* smaller, justifying this assumption. The operators then depend only on spin and isospin variables, and the spatial integrals lead to a pair distribution function,

$$\rho(\mathbf{x}',\mathbf{x}) = \langle 0 | \delta(\mathbf{x}-\mathbf{z}_\alpha)\delta(\mathbf{x}'-\mathbf{z}_\beta) | 0 \rangle.$$

[21] B. Lippmann and J. Schwinger, Phys. Rev. **79**, 469 (1950).
[22] G. Takeda and K. M. Watson, Phys. Rev. **97**, 1336 (1955).
[23] A. K. Kerman, H. McManus and R. M. Thaler, Ref. 14.
[24] N. C. Francis and K. M. Watson, Ref. 8.
[25] H. P. Stapp, T. J. Ypsilantis, and N. Metropolis, Phys. Rev. **105**, 302 (1957).

The assumption of Lax and Feshbach,[26] that the distributions differ only in space-symmetric and space-antisymmetric states, is made. With further simplifications involving assumptions of large nuclei, high incident energy and angular symmetry, the effect of correlations is contained[15] in two correlation lengths, $R_{s,a}$, for the space symmetric and antisymmetric states, respectively. If one knows the nuclear wave functions, $R_{s,a}$ can be calculated. In the Johnston-Watson work, values obtained from assuming a Fermi-gas model for the nucleus and from wave functions given by Brueckner and Gammel[27] are used. Thus for the Fermi gas model, one has[15]

$$R_s+R_a=-24\pi/[5(A+4)k_F],$$
$$R_s-R_a=6\pi A/[5(A+4)k_F],$$

where k_F is the Fermi momentum, ~ 1.27 F^{-1}. The Brueckner-Gammel calculation yields

$$R_s=R_a=-0.84 \text{ F},$$

so that the contributions to $V^{(2)}$ are quite different for the two cases. These are taken as typical values of the correlation lengths in the present calculations. The effect of varying them as arbitrary parameters is also studied. The spin and isospin sums lead to contributions to V_{op} from all terms of the scattering matrix, Eq. (7).[15]

In coordinate space the resulting potential may be written

$$V_{\text{op}}=V^{(1)}+V^{(2)}=V_c^{(1)}+V_c^{(2)}+(V_s^{(1)}+V_s^{(2)}), \quad (8)$$

where

$$V_c^{(1)}(r)=-(A/\pi\epsilon_0)(k_L/k_c)\int q^2dq\, F(q)j_0(qr) \times[A_0(q)\pm(2T_3/A)A_\tau(q)],$$
$$V_s^{(1)}(r)=-(A/i\pi\epsilon_0)(k_L/k_ck)(1/r)\int q^2dq\, F(q)j_1(qr) \times[C_0(q)\pm(2T_3/A)C_\tau(q)]/[1-q^2/4k^2]^{1/2}, \quad (9)$$

and

$$V_c^{(2)}(r)=(2\pi^2/ik\epsilon_0)(A^2/V_A)(k_L/k_c)^2 \times[(R_s+R_a)g_d+(R_s-R_a)g_e]\rho(r),$$
$$V_s^{(2)}(r)=(2\pi^2/k\epsilon_0)(A^2/V_A)(k_L/k_c)^2(1/kk_c) \times[(R_s+R_a)h_d+(R_s-R_a)h_e]\frac{1}{r}\frac{d\rho}{dr}. \quad (10)$$

In these equations, which follow the Johnston[15] notation, $A_{0,\tau}(q)$ and $C_{0,\tau}(q)$ are linear combinations of the first two scattering amplitudes of Eq. (7) for isospin singlet and triplet states of two nucleons, while $g_{d,e}$ and $h_{d,e}$ involve forward angle values of all the amplitudes in Eq. (7). The quantity T_3 is the third component of isotopic spin, V_A is the nuclear volume, k_L the laboratory nucleon incident wave number, k_c its value in the two-nucleon barycentric system and k the value in the nucleon-nucleus systems; ϵ_0 is the total energy of the incident nucleon in the Nc.m. system. The form factor $F(q)$ is

$$F(q)=\int \rho(r)e^{-iq\cdot r}d^3r, \quad (11)$$

where $\rho(r)$ is normalized so that

$$\int \rho(r)d^3r=1.$$

In the first-order potentials, Eq. (9), the integrals over q involve the "spherical Bessel functions" $j_0(qr)$ and $j_1(qr)$; if $A_{0,\tau}(q)$ and $C_{0,\tau}(q)$ are replaced by their values for $q=0$, the integrals lead to $\rho(r)$ and $d\rho(r)/dr$, respectively. The potential would then have the same radial form as Eq. (1).

A further correction, of order $1/A$, is necessary because of terms in the second order potential not included in Eq. (10). These may be included by V_{op} by a factor

$$\gamma=1-(1/A)+\Delta[(V_A/8\pi^3)(V_1+V_2)]^{-2}, \quad (12)$$

where Δ, V_1, V_2 are combinations of scattering amplitudes.[28] Nucleon-nucleus scattering amplitudes obtained from the potential modified by a factor γ must be divided by γ to give the desired cross section.

The present calculation of the potential utilized the Yale phase-parameters[17,18] for the two-nucleon matrix. A comparison with the Johnston calculation,[15] based on phases from the Gammel-Thaler potential,[19] is facilitated by writing the potential in his form (assuming the forward-angle approximation):

$$U=\lambda^{-3}\left[U_{00}+\frac{1}{A}U_{01}\pm\frac{T_3}{A}U_{02}\right] +\lambda^{-6}(R_s+R_a)\left[U_{10}+\frac{1}{A}U_{11}\pm\frac{T_3}{A}U_{12}\right] +\lambda^{-6}(R_s-R_a)\left[U_{20}+\frac{1}{A}U_{21}\pm\frac{T_3}{A}U_{22}\right], \quad (13)$$

and similarly for W, where U replaces (U_c+iW_c) in Eq. (1), and W replaces (U_s+iW_s); $\lambda=R_AA^{-1/3}/$

[26] M. Lax and H. Feshbach, Phys. Rev. **81**, 189 (1951).
[27] K. Brueckner and J. Gammel, Phys. Rev. **109**, 1023 (1958).

[28] R. R. Johnston, Nucl. Phys. **36**, 368 (1962). The authors wish to thank Dr. Johnston for a correspondence concerning the form of Δ. The published form contains a misprint which has no numerically significant consequences on Dr. Johnston's calculations reported in the reference.

TABLE I. Parameters of the theoretical optical potential, in the Johnston[a] notation. The phase parameters of Breit *et al.*[b] and Hull *et al.*[c] are used for the nucleon-nucleon amplitudes.

	95 MeV		156 MeV		300 MeV		350 MeV	
	Re	Im	Re	Im	Re	Im	Re	Im
U_{00} (MeV)	−38.12	−30.41	−24.79	−25.94	− 5.07	−25.94	− 1.08	−26.96
U_{01} (MeV)	52.76	−23.58	76.28	−41.52	− 5.42	−29.96	−28.13	−25.86
U_{02} (MeV)	12.23	25.06	5.26	16.02	−10.00	10.53	−13.82	11.45
U_{10} (MeV F^{-1})	14.09	− 3.21	6.36	0.29	1.03	2.52	0.22	2.69
U_{11} (MeV F^{-1})	−31.04	39.91	−12.78	30.78	3.83	8.83	6.61	6.17
U_{12} (MeV F^{-1})	−16.13	− 3.59	− 5.27	− 2.82	1.61	− 2.52	2.67	− 2.40
U_{20} (MeV F^{-1})	− 6.69	5.83	− 2.02	4.03	0.67	1.48	0.92	0.92
U_{21} (MeV F^{-1})	53.85	23.07	17.30	− 6.12	4.85	11.80	2.71	10.77
U_{22} (MeV F^{-1})	10.56	3.48	5.04	1.19	− 0.40	1.56	− 1.24	1.85
W_{00} (MeV)	3.940	− 1.134	3.070	− 0.678	2.156	− 0.468	2.001	− 0.466
W_{01} (MeV)	− 0.951	4.765	− 0.354	7.594	2.491	− 0.504	1.532	− 2.474
W_{02} (MeV)	1.353	1.689	0.896	1.285	− 0.178	0.654	− 0.456	0.611
W_{10} (MeV F^{-1})	− 0.465	1.122	− 0.310	0.463	− 0.209	0.090	− 0.198	0.055
W_{11} (MeV F^{-1})	1.050	− 2.259	− 0.848	− 1.490	− 0.094	− 0.018	0.014	0.179
W_{12} (MeV F^{-1})	− 0.125	− 0.464	− 0.047	− 0.189	− 0.112	− 0.005	0.152	0.020
W_{20} (MeV F^{-1})	− 0.030	− 0.290	0.009	− 0.118	0.037	− 0.030	0.039	− 0.019
W_{21} (MeV F^{-1})	− 1.539	4.615	− 0.970	1.948	− 0.792	0.326	− 0.772	0.160
W_{22} (MeV F^{-1})	0.095	0.713	0.088	0.386	− 0.005	0.130	− 0.028	0.087

[a] See Ref. 15.
[b] See Ref. 17.
[c] See Ref. 18.

(1.2 F), with R_A the nuclear radius. The relation between the forms in Eqs. (9), (20) and Eq. (13) may be obtained by straightforward comparison.[29] The plus sign in Eq. (13) refers to incident protons, the minus sign to incident neutrons, respectively. Table I contains values of the coefficients U_{ij} and W_{ij} and may be compared to the table of Johnston.[15] Only the first terms of the first-order coefficients are similar; Bethe[10] has pointed out that this is to be expected from any sets of phase parameters which generally fit the total cross section in nucleon-nucleon scattering.

Nucleon distributions have been used which yield analytic forms for the form factors. This is a matter of convenience in evaluation of the first-order potentials and is justified by the electron scattering experiments, which are insensitive to reasonable distribution functions so long as the radial and surface parameters R_h and t_s are the same.[5] Specifically, the result of Ehrenberg *et al.*[30] was used for carbon, and the Gaussian-uniform shape introduced by Helm[31] for Al, Fe, Cu, Pb, with constants adjusted to the R_h, t_s values for specific nuclei given by Hofstadter[5] or interpolated among his values. The calculation of the first-order potential then involves a numerical evaluation of Eq. (9). The integrals over q were cut off at $q=2k_c$, since this is the limit of momentum transfer in the free two-nucleon case, and the input scattering amplitudes are not defined beyond this point. Apart from the assumption that nothing drastic happens to the scattering amplitude in the nonphysical region of the free two-nucleon case to give sizable contributions to the integrals for $q>2k_c$, it was clearly necessary to check that the decrease of $F(q)$ was sufficiently rapid so that use of the integrals was reasonable. A test of this point was made by numerical evaluation of the integrals assuming constant amplitudes to see whether the integral when cut off at $2k_c$ would closely reproduce $\rho(r)$ and $d\rho/dr$. The Hill-Ford distribution[32] fails this test, due to its having no exponentially decreasing part, so that it was not used even though it has an analytic form factor. The distribution chosen is satisfactory, although some errors occur in the potential at small distances. The small-angle scattering of interest here is caused predominantly by the long-range part of the potential, and it has been confirmed by direct calculation that the errors in the potential do not affect the observables in the angular range studied.

The parameters entering the calculation may now be summarized: the phase parameters used to calculate the elements of the two-nucleon scattering matrix are from the Yale study[17,18] with one-pion phase parameters included; the nucleon distribution function is taken from electron scattering experiments[5,30] and the initial values of the correlation lengths from specific models of nuclear matter.[15] None of these was derived from the phenomenon to be studied. Since the real and imaginary parts of the scattering matrix do not have the same dependence on q, the first-order potential, Eq. (9), will have different radial and thickness parameters for the real and imaginary parts, and each may be different from $\rho(r)$ itself. The second-order central potential at any energy is of the form const$\times\rho(r)$, so its principal effect is to change the potential depth, although clearly not simply by a multiplicative factor.

The most straightforward comparison with phenomenological results can be made in terms of volume integrals[23] of the potentials, since differences in choice

[29] F. A. McDonald, thesis, Yale University, 1965 (unpublished).
[30] H. F. Ehrenberg, R. Hofstadter, U. Meyer-Berkout, D. G. Ravenhall, and S. E. Sobottka, Phys. Rev. **113**, 666 (1959).
[31] R. H. Helm, Phys. Rev. **104**, 1466 (1956).
[32] D. L. Hill and K. W. Ford, Phys. Rev. **84**, 1617 (1954).

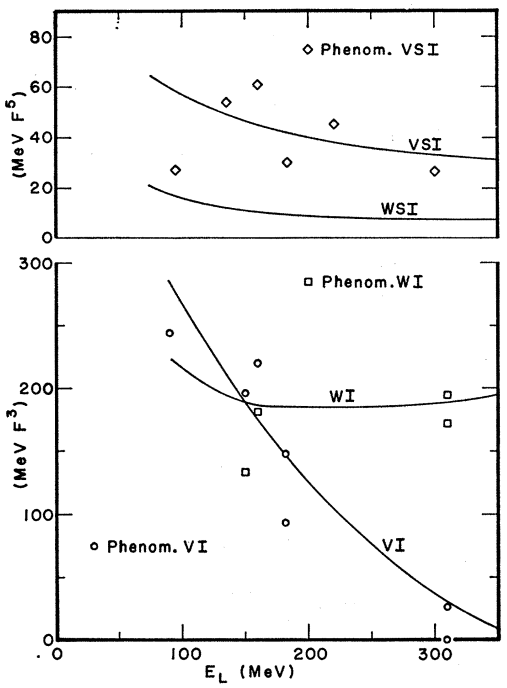

FIG. 1. Volume integrals of the first-order theoretical optical potential, as defined in Eq. (14), compared with phenomenological values taken from Hodgson.[4] The values shown are for nuclei with $N=Z$ such as carbon. Note that the negative of WSI is shown.

of form of $\rho(r)$ are eliminated, dependence on A is minimized. In Fig. 1 is shown the volume integral of the first-order potential as a function of incident-nucleon energy, with

$$\begin{aligned}\mathrm{VI}+i\mathrm{WI}&=-\frac{1}{A}\int V_c^{(1)}(r)d^3r\\&=-\frac{4\pi}{3}(1.2)^3U_{00}\\&=-7.23U_{00},\\\mathrm{VSI}+i\mathrm{WSI}&=\frac{1}{A}\int V_s^{(1)\prime}(r)d^3r\\&=14.46W_{00},\end{aligned}\qquad(14)$$

where

$$V_s^{(1)}(r)=\frac{1}{r}\frac{d}{dr}V_c^{(1)\prime}(r).$$

Here $T_3=0$, i.e., the nucleus has $N=Z$. The final relations of Eq. (14) are *not* dependent on using the forward-angle approximation for $V_c^{(1)}(r)$ and $V_s^{(1)}(r)$. Phenomenological results, tabulated by Hodgson,[4] are shown for comparison except for the imaginary spin-orbit part, where phenomenological values are small in agreement with theoretical ones but scatter too much for useful presentation. The refinement of taking into account neutron excess as well as effects of second-order potentials could easily be included theoretically, but the scatter of phenomenological values makes this unfruitful. The general trend of the phenomenological values is reproduced theoretically, as has been the experience with earlier analyses,[14] but the detailed variations are not given. That deviations from theory, especially for VSI, are essential in fitting some data will be discussed later.

The effect of including the q dependence of the two-nucleon scattering matrix in the first-order potential is illustrated in Figs. 2 and 3, for the case of protons incident on aluminum. For the imaginary central potential over the whole energy range (~100–350 MeV), and for the real central potential at the lower energies, the depth at $r=0$ is reduced and the potential tail is extended, compared to the values for the forward-angle approximation. The depth at $r=0$ of the (relatively small) real central potential at 300 MeV is

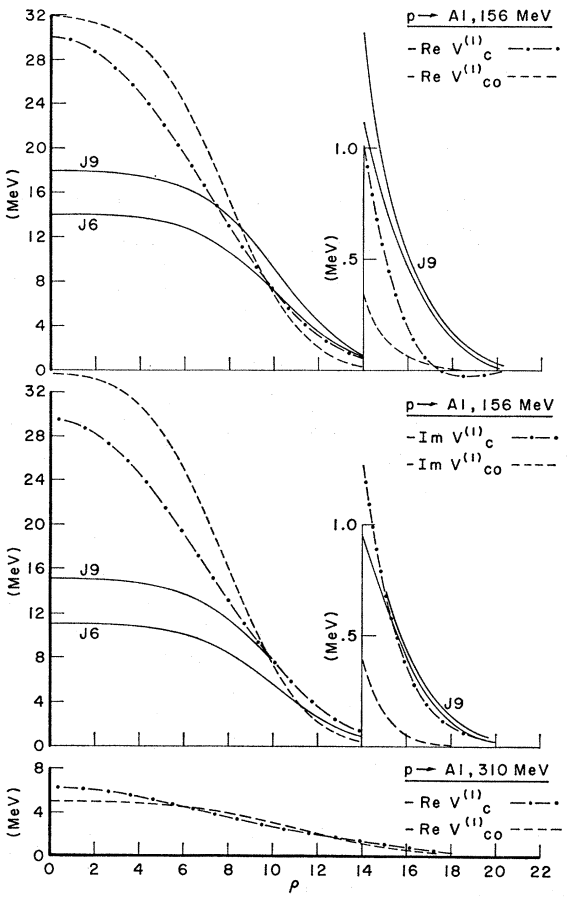

FIG. 2. The first-order central potential for protons incident on aluminum, comparing the integrated potential $V_c^{(1)}$ with the potential $V_{c0}^{(1)}$, which employs the forward-angle approximation. Curves *J6* and *J9* are phenomenological potentials of Johansson *et al.* (Ref. 33). The negative of the potential is shown in each case. The quantity $\rho=kr$.

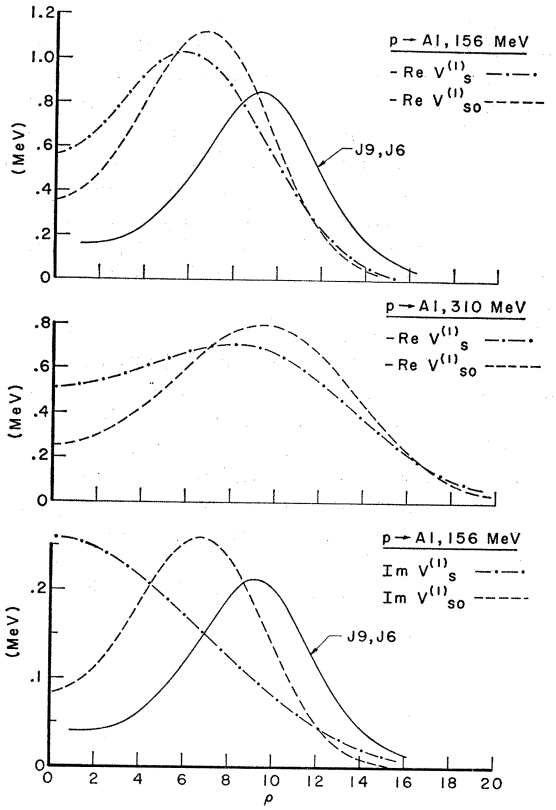

FIG. 3. The first-order spin-orbit potential, for protons incident on aluminum, comparing the integrated potential $V_s^{(1)}$ with the potential $V_{s0}^{(1)}$, which employs the forward-angle approximation. Curves *J*6 and *J*9 are phenomenological potentials of Johansson *et al.* (Ref. 33). The negative of the real potential is shown. Note the enlarged scale on the ordinate for $\mathrm{Im}V_s^{(1)}$.

increased slightly. Also shown are phenomenological potentials obtained by Johansson *et al.*[33] for a range of moderate-mass nuclei, with radial dependence given by the Woods-Saxon shape. A potential having a volume integral given in Fig. 1, but with the same Woods-Saxon shape as *J*6 and *J*9, would have depths at $r=0$ of -16.7 and -17.4 MeV, for real and imaginary central potentials, respectively. The peak of the real spin-dependent potential is reduced and shifted from that in forward-angle approximation. The imaginary spin-dependent potential is negligible in all cases.

Effects of further modifications may be sampled in Fig. 4. The theoretical potentials are for neutrons on copper at 156 MeV. The contribution of the second-order potential, with both choices of correlation lengths, is shown, and the effect of radically varying the phase parameters is shown by computing potentials with the Gammel-Thaler (GT) values. Only the Brueckner-Gammel correlation lengths are used for the second-order contribution with the Gammel-Thaler phase parameters. The imaginary first-order central potentials

[33] A. Johansson, G. Tibell, K. Parker, and P. E. Hodgson, Nucl. Phys. **21**, 383 (1960).

TABLE II. Shape parameters for the first-order potential. Phenomenological values are taken from Refs. 5 and 6. Quantities given are defined and discussed in the text.

Target nucleus		C		Al		Fe	
E_{lab} (MeV) (protons incident)		156	310	156	310	156	310
Potential	Shape parameters	Values of shape parameters (F)					
Phenom.[a]							
$\mathrm{Re}V_c$ and	R_h			3.75	3.75	4.79	4.79
$\mathrm{Im}V_c$	t_s			2.86	2.86	2.86	2.86
Phenon.[b]	R_h			3.3			
$\mathrm{Re}V_c$	t_s			2.9			
	R_h			4.2			
$\mathrm{Im}V_c$	t_s			2.9			
$\mathrm{Re}V_{c0}^{(1)}$	R_h	2.30	2.30	2.95	2.95	4.06	4.06
$\mathrm{Im}V_{c0}^{(1)}$	t_s	2.05	2.05	2.70	2.70	2.48	2.48
$\mathrm{Re}V_c^{(1)}$	R_h	2.27	1.48	2.79	2.39	3.82	3.75
	t_s	2.86	3.15	3.43	3.51	3.55	3.06
$\mathrm{Im}V_c^{(1)}$	R_h	2.21	2.15	2.80	2.85	3.83	3.92
	t_s	3.07	2.85	3.54	3.24	3.63	3.24
$\mathrm{Re}V_s^{(1)}$	R_m, F	1.03	1.51	2.17	2.17	3.60	3.62
$\mathrm{Re}V_{s0}^{(1)}$	R_m, F	1.80	1.80	2.50	2.50	3.80	3.80
$(\mathrm{Re}V_c^{(1)}/\mathrm{Re}V_{c0}^{(1)})_{r=0}$		0.82	1.32	0.94	1.24	1.00	1.09
$(\mathrm{Im}V_c^{(1)}/\mathrm{Im}V_{c0}^{(1)})_{r=0}$		0.78	0.92	0.88	0.93	0.95	0.98
$(\mathrm{Re}V_s^{(1)})_{\max}/(\mathrm{Re}V_{s0}^{(1)})_{\max}$		0.88	0.85	0.92	0.89	0.87	0.85

[a] Reference 5.
[b] Reference 6.

for the two sets of phase parameters are quite similar, reflecting the fact that the total nucleon-nucleon cross section strongly influences the part of the scattering matrix contributing to $\mathrm{Im}V_c^{(1)}$.

In Table II are shown the range and surface parameters for $V_c^{(1)}$ and $V_{c0}^{(1)}$ for sample cases to show the effect of q dependence of the two-nucleon scattering matrix, together with phenomenological results for comparison. The summary of Hofstadter[5] supplied the phenomenological shape parameters in which real and imaginary parts of the potential have the same values, and the analysis of Hodgson[6] the results for aluminum at medium energies (actually about 160 MeV) in which the possibility of having different ranges for the real and imaginary parts was examined. The latter refinement allowed behavior at diffraction minima for the cross section to be more faithfully reproduced. While the present approximation would not be expected to hold at larger angles where higher order multiple scatterings could contribute, the influence of the q dependence of the two nucleon scattering matrix is to give different shape parameters for the real and imaginary potentials. Included also in Table II are values of the radius R_m, at which the real spin-orbit potential reaches maximum, for both $V_s^{(1)}$ and $V_{s0}^{(1)}$, ratios of depths of the central potentials $V_c^{(1)}$ and $V_{c0}^{(1)}$ at $r=0$, and ratios of maximum values of the real spin-orbit potentials.

The trends of the shape parameters with energy and mass number as shown in Table II are typical of all the calculations of this study, especially in the striking

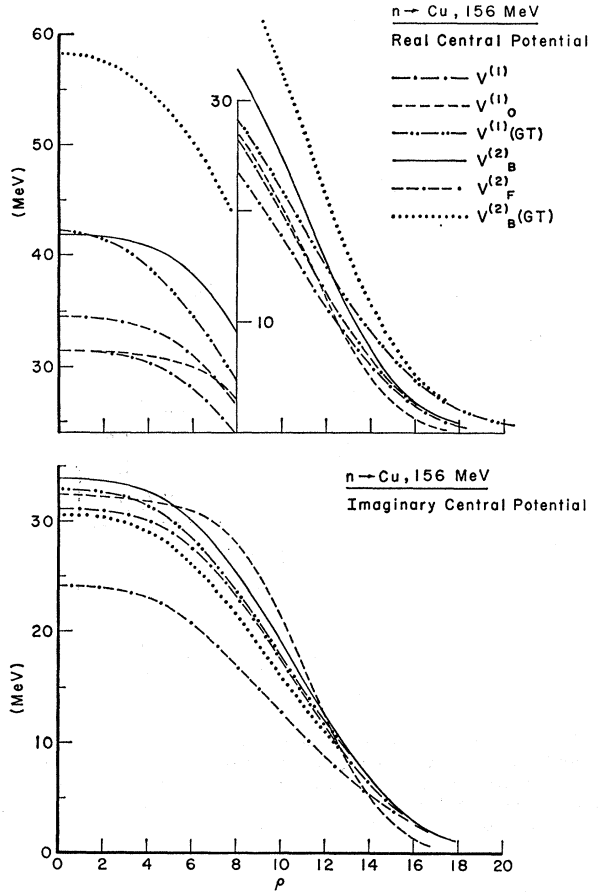

FIG. 4. The theoretical central potential for neutrons incident on copper, showing all potential approximations: $V^{(1)}$, the integrated first-order potential, Eq. (9); $V_0^{(1)}$, the first-order potential in forward-angle approximation; $V_B^{(2)}$ and $V_F^{(2)}$, the *sum* of $V^{(1)}$ and the second-order potentials of Eq. (10), with Brueckner-Gammel (Ref. 27) and Fermi gas correlation lengths, respectively. The designation GT denotes use of Gammel-Thaler (Ref. 19) phase parameters in place of those of the Yale group (Refs. 17, 18). The negative of the potential is shown.

point illustrated by the entries: the surface thickness t_s is much more strongly effected by inclusion of the angular variation of the two nucleon scattering matrix than is R_h, the radius at half-maximum. Compared to the value of R_h for the nucleon distribution itself; i.e., for $V_{c0}^{(1)}$, the value for the integrated potential is always smaller, though by amounts ranging only from a few to 10% (except for carbon at 310 MeV). On the other hand, t_s is larger for the integrated potential by as much as 50%. An rms radius for $V_c^{(1)}$ would exceed that for the nucleon distribution, therefore, but because of an increase in t_s rather than R_h. Schenter and Downs[34] have noted the importance of the surface effect, while Kerman *et al.*[23] assumed that the radial parameter was most important—a conclusion not supported by these calculations. The increased radial parameter for the imaginary part required by Hodgson[6] and Johannson *et al.*[35] is exhibited in several cases by the integrated potentials, but by nothing like the phenomenological amount. No difference in t_s was found necessary by these investigators (the possibility of varying t_s as well as R_h on an equal footing was apparently not thoroughly explored).

Although the first- and second-order potentials have somewhat different radial dependence, the principal effect of the second-order potential may be seen by comparing the potential depths at $r=0$. This is shown for neutrons on copper for a few energies in Table III

TABLE III. Ratio of second-order potential to first-order potential at $r=0$, for neutrons incident on copper. The labels B and F indicate that correlation lengths are taken from Brueckner-Gammel and Fermi-gas models of the nucleus, respectively.

E_{lab} (MeV)	$(\mathrm{Re}V_c^{(2)}/\mathrm{Re}V_c^{(1)})_{r=0}$		$(\mathrm{Im}V_c^{(2)}/\mathrm{Im}V_c^{(1)})_{r=0}$	
	B	F	B	F
95	0.50	0.25	−0.15	−0.30
156	0.33	0.10	0.10	−0.25
300	0.30	−0.15	−0.20	−0.07
350	0.60	−0.50	0.20	−0.03

for the central potentials. The labels B and F indicate that the Brueckner-Gammel or Fermi gas models of nuclei have been used for the correlation lengths $R_{s,a}$ which enter Eq. (10). Although the percentage changes in the real part of $V_c^{(1)}$ are quite large at high energies, the size of the potential is small compared to the imaginary part, so that effects on observables are not large.

III. COMPARISON WITH DATA

A. Differential Cross Section

The differential cross section and polarization in nucleon-nucleus scattering are now calculated from the potential discussed in Sec. II. Phase shifts are obtained by numerical integration of the Schrödinger equation on a digital computer; a portion of the SCAT4 program[36] was used here. The data used for comparison in the present work are indicated in Table IV. Only tabulated data were used, and the energy given is that at which the calculations were made; the experimental energies may differ by one or two MeV. For comparison with data for protons incident, a Coulomb potential was added to the nuclear potential of Eqs. (9) and (10). Since the $1/r$ tail of this potential is the dominant feature, the potential corresponding to a uniform charge distribution was employed. A Coulomb spin-orbit term caused by the magnetic moment interaction[37] was also

[34] R. E. Schenter and B. Downs, Phys. Rev. **129**, 2292 (1963).

[35] A. Johansson, U. Swanberg, and R. E. Hodgson, Ref. 14.

[36] M. A. Melkanoff, D. S. Saxon, J. S. Nodvik, and D. G. Cantor, *A Fortran Program for Elastic Scattering Analyses with the Nuclear Optical Model* (University of California Press, Los Angeles, 1961).

[37] W. Heckrotte, Phys. Rev. **101**, 1406 (1956).

TABLE IV. Sources of data used for comparison with theory. Some comparisons have been omitted from presentation here (in Figs. 5–16), where no new information would have been illustrated.

Energy (MeV)	Targets	Data type	Reference
	Elastic neutron scattering		
84	Al, Cu, Pb	σ	a
95	C, Al, Cu, Pb	σ	b
137	C, Al, Cu, Pb	σ	c
156	C, Al, Cu, Pb	σ, P	d
300	C, Al, Cu, Pb	σ	e
350	C, Al, Cu, Pb	σ	f
350	C, Al, Cu, Pb	P	g
	Elastic proton scattering		
95	C	σ, P	h
137	C	σ, P	i
156	C, Fe	P	j
156	Al	σ, P	k
180	C, Al, Fe	σ	l
200	C	σ, P	m
300	C, Al, Fe	σ, P	n

[a] A. Bratenahl, S. Fernbach, R. H. Hildebrand, C. E. Leith, and B. T. Moyer, Phys. Rev. **77**, 597 (1950).
[b] G. L. Salmon, Nucl. Phys. **21**, 15 (1960).
[c] C. P. Van Zyl, R. G. P. Voss, and R. Wilson, Phil. Mag. **1**, 1003 (1956).
[d] R. S. Harding, Phys. Rev. **111**, 1164 (1958).
[e] W. P. Ball, UCRL-1938 (unpublished).
[f] A. Ashmore, D. S. Mather, and S. K. Sen, Proc. Phys. Soc. (London) **71**, 552 (1958).
[g] R. T. Siegel, Phys. Rev. **100**, 437 (1955).
[h] J. M. Dickson and D. C. Salter, Nuovo Cimento **6**, 235 (1957).
[i] J. M. Dickson and D. C. Salter, Ref. h, above.
[j] R. Alphonce, A. Johansson, and G. Tibell, Nucl. Phys. **4**, 672 and 643 (1957).
[k] A. Johansson, G. Tibell, K. Parker, and R. E. Hodgson, Nucl. Phys. **21**, 383 (1960).
[l] A. Johansson, U. Swanberg, and P. E. Hodgson, Arkiv Fysik **19**, 541 (1961).
[m] T. T. Thwaites, Ann. Phys. (N. Y.) **12**, 56 (1961).
[n] O. Chamberlain, E. Segrè, R. D. Tripp, C. Wiegand, and T. J. Ypsilantis, Phys. Rev. **102**, 1659 (1956).

used, but its contribution to the polarization is numerically insignificant.

The scattering of neutrons provides the clearest test of the theory, since Coulomb scattering does not obscure the effects of potential variations at small angles. Figures 5 and 6 show the results for all potential types in four sample cases, and Figs. 7–11 give a more nearly complete survey. The extension of the potential tail and change in depth of the integrated first order potentials compared to those calculated in forward-angle approximation (for the two-nucleon matrix) result in a narrower diffraction pattern and increased small-angle cross section, i.e., a "rotation" of the calculated cross-section curve. This rotation gives an improvement in fitting the angular dependence of $\sigma(\theta)$ in every instance, although not always as great as required by the data. The addition of the second-order potential shows up principally as a shift in level of the cross section. Use of Brueckner-Gammel correlation lengths usually results in improved agreement with data, since the second-order potential computed with them raises the cross section. Although at the higher energies, this shift leaves the theoretical result still low, the curves labeled $V_B^{(2)}$, meaning that all refinements discussed here have been included and Brueckner-Gammel (BG) correlation lengths used for

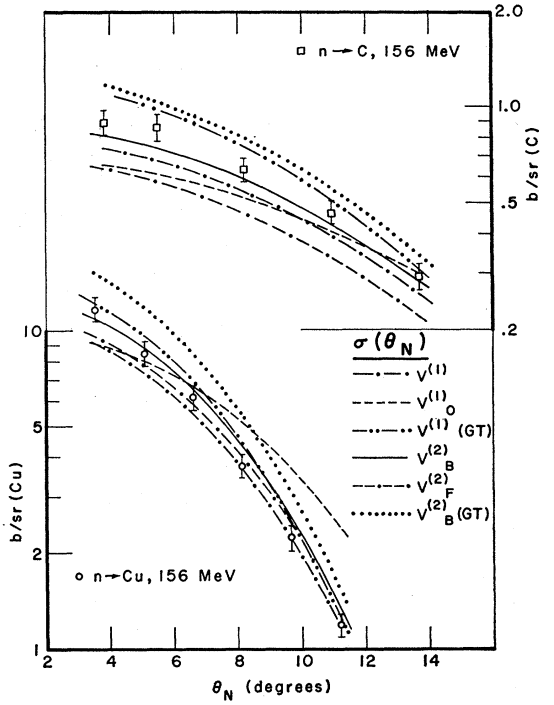

FIG. 5. Differential cross-section data for neutrons incident on C and Cu at 156 MeV, compared with theoretical predictions. θ_N is the scattering angle in the nucleon-nucleus center-of-mass (Nc.m.) system. Curves are labeled by the potential designation; see caption of Fig. 4. See also the potentials in Fig. 4.

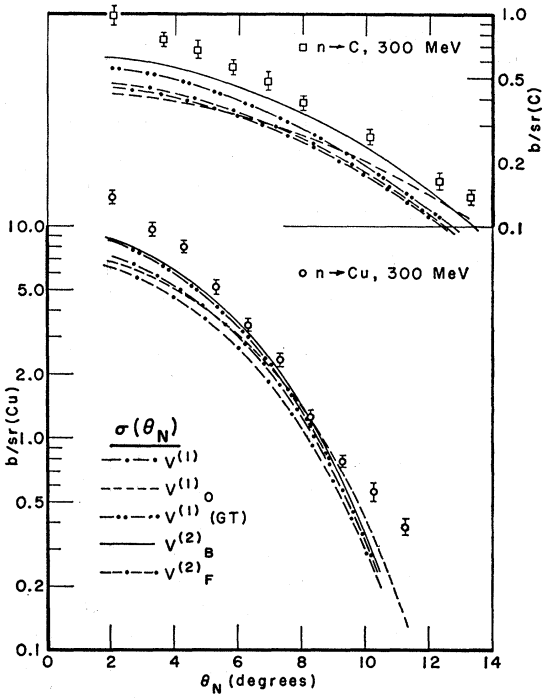

FIG. 6. Differential cross-section data for neutrons incident on C and Cu at 300 MeV, compared with theoretical predictions. Notation is that of Fig. 5.

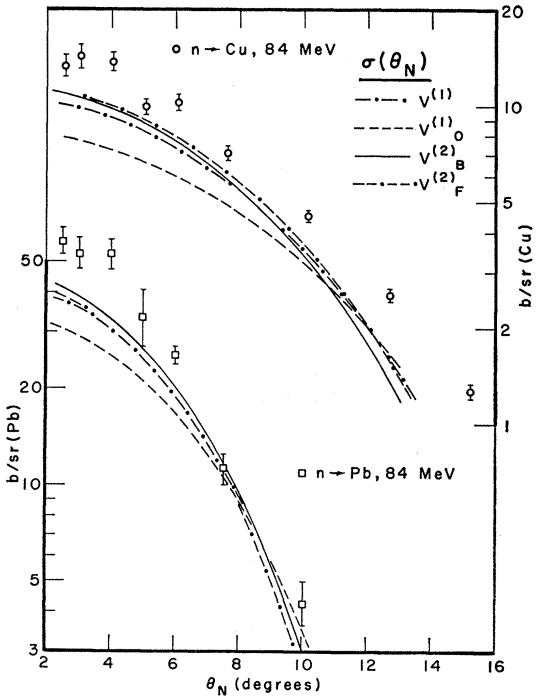

FIG. 7. Differential cross-section data for neutrons incident on Cu and Pb at 84 MeV, compared with theoretical predictions. Notation is that of Fig. 5.

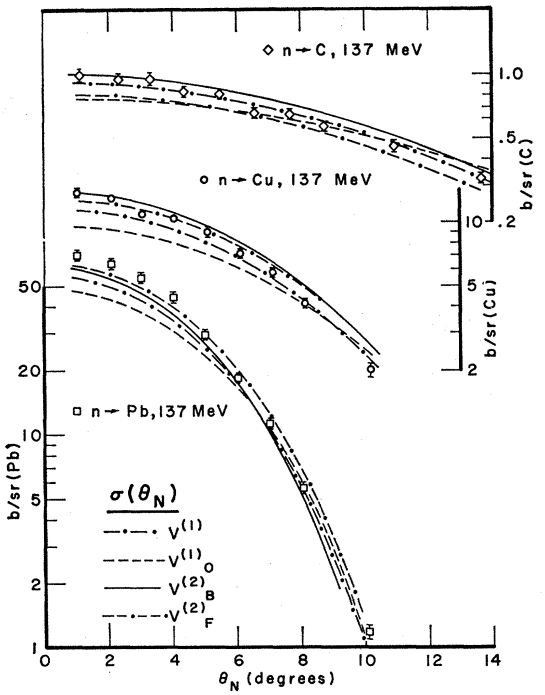

FIG. 9. Differential cross-section data for neutrons incident on C, Cu, and Pb at 137 MeV, compared with theoretical predictions. Notation is that of Fig. 5.

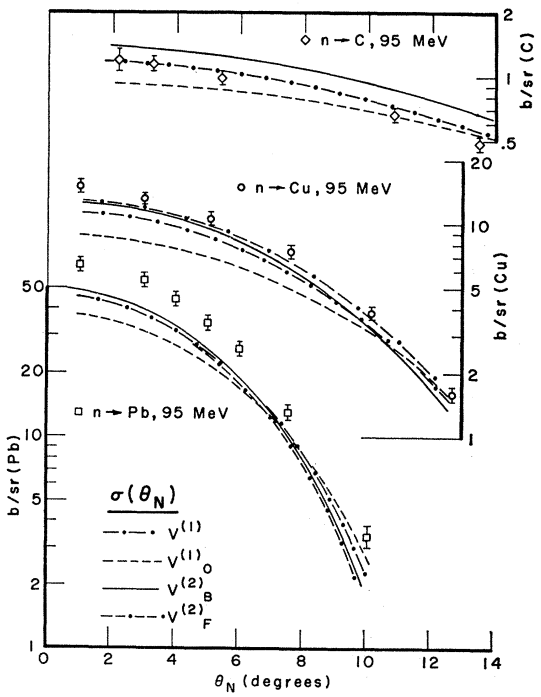

FIG. 8. Differential cross-section data for neutrons incident on C, Cu, and Pb at 95 MeV, compared with theoretical predictions. Notation is that of Fig. 5.

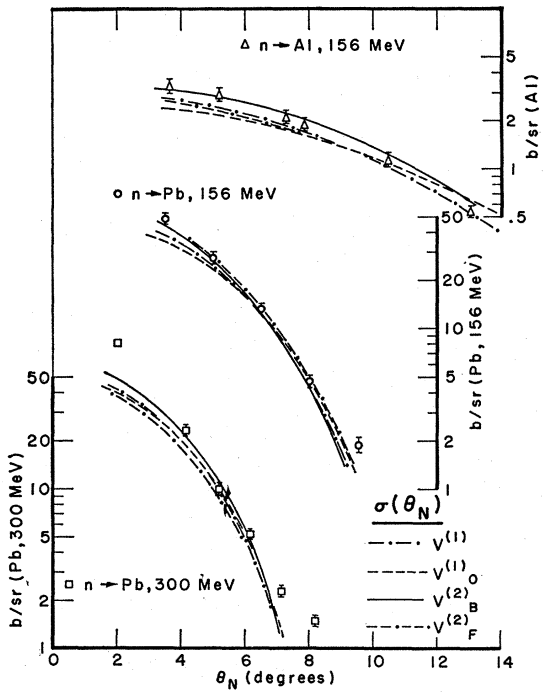

FIG. 10. Differential cross-section data for neutrons incident on Al and Pb at 156 MeV, and on Pb at 300 MeV, compared with theoretical predictions. See also Figs. 5 and 6. Notation is that of Fig. 5.

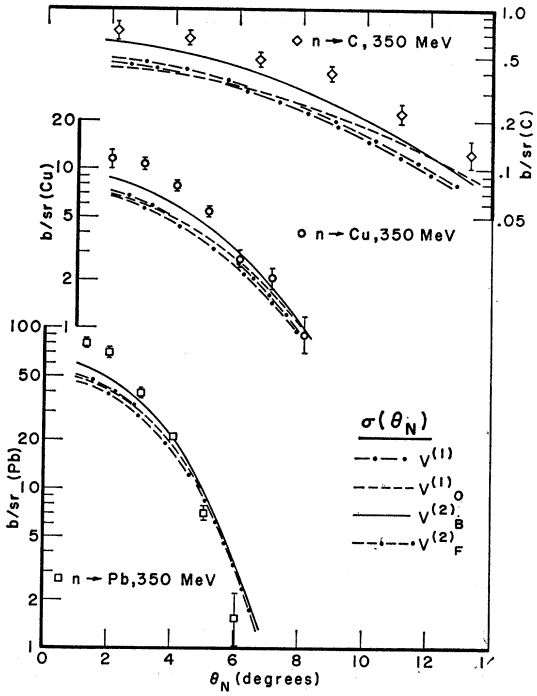

FIG. 11. Differential cross-section data for neutrons incident on C, Cu, and Pb at 350 MeV, compared with theoretical predictions. Notation is that of Fig. 5.

$R_{s,a}$, give the best of the theoretical fits. Cross sections predicted from potentials using Fermi gas correlation lengths are consistently low in this range. At lower energies the preference for BG correlation lengths is not so clear; the predictions from the $V_F^{(2)}$ potentials are too low for light nuclei, but are larger than those for $V_B^{(2)}$ for heavy targets, and provide at least an equally good fit to data. One should emphasize at this point the over-all good quality of the data fits illustrated in Figs. 5–11 (and subsequently), despite the fact that no arbitrary parameters have been used in the calculation.

It may also be noted that the use of Gammel-Thaler (GT) phase parameters for the two-nucleon scattering matrix provides in the $V_B^{(2)}$ approximation, a fit to data of reasonable character, although the regularities noted above do not appear: the theoretical cross sections are sometimes larger, sometimes smaller than the experimental ones (see Figs. 5 and 6). These calculations, therefore, are relatively insensitive to the two-nucleon phase-parameters. While on the basis of the whole survey they tend to rule out the GT fit, they could not be used to select among several good fits to nucleon-nucleon data.

Proton-nucleus scattering is illustrated in Figs. 12 and 13. The treatment of the Coulomb interaction appears adequate, as the lowest angle data are well fitted in all approximations. At 95 and 137 MeV, the proton-carbon theoretical cross sections are all large compared to experiment,[38] the only such cases. In this regard, it should be noted that Gerstein *et al.*[39] report results 25–35 percent greater at 95 MeV. Also, comparison with data for neutrons incident (see Fig. 8) shows that Coulomb effects have accounted for only half the experimental differences; the nuclear potentials are identical for neutrons and protons incident, since $T_3=0$ for carbon. It is possible, therefore, that the experimental normalization of the cross-section data shown is in error. Comparison of theoretical and experimental values for the other cases again supports the superiority of the $V_B^{(2)}$ potential, although Coulomb effects obscure the differences. The curves marked *J*6, *J*9 in Fig. 12 are predictions from the phenomenological potentials of Johansson *et al.*[33], which were shown in Figs. 2 and 3. Although *J*6 and *J*9 give poorer fits than the other curves, it should be pointed out that they were determined[33] by fitting data for a range of nuclei, not just aluminum, and the treatment of Coulomb effects may have differed.

B. Polarization

Nucleon-nucleus polarization provides the severest test of the theory, and emphasizes the importance of having data over a range of energies and targets.

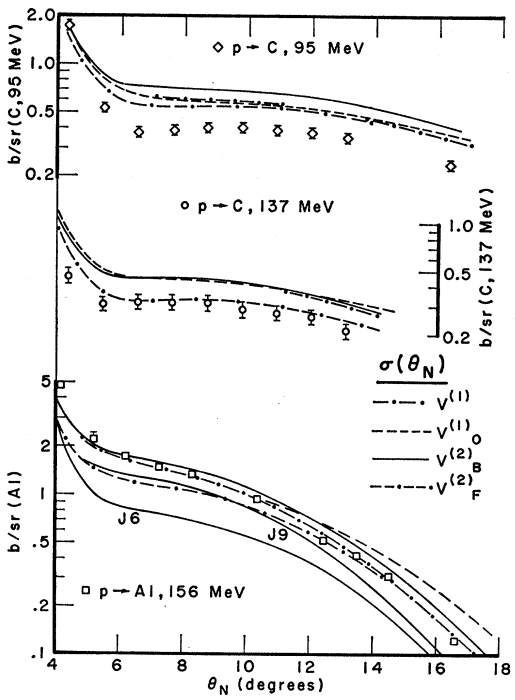

FIG. 12. Differential cross-section data for protons incident on C at 95 and 137 MeV, and on Al at 156 MeV, compared with theoretical predictions. Notation is that of Fig. 5. The curves *J*6 and *J*9 correspond to phenomenological results of Johansson *et al.* (Ref. 33). Compare also the potentials in Figs. 2 and 3.

[38] J. M. Dickson and D. C. Salter, Nuovo Cimento **6**, 235 (1957).
[39] G. Gerstein, J. Niederer, and K. Strauch, Phys. Rev. **108**, 427 (1957); see also G. L. Salmon, Nucl. Phys. **21**, 15 (1960) for results with neutrons at this energy.

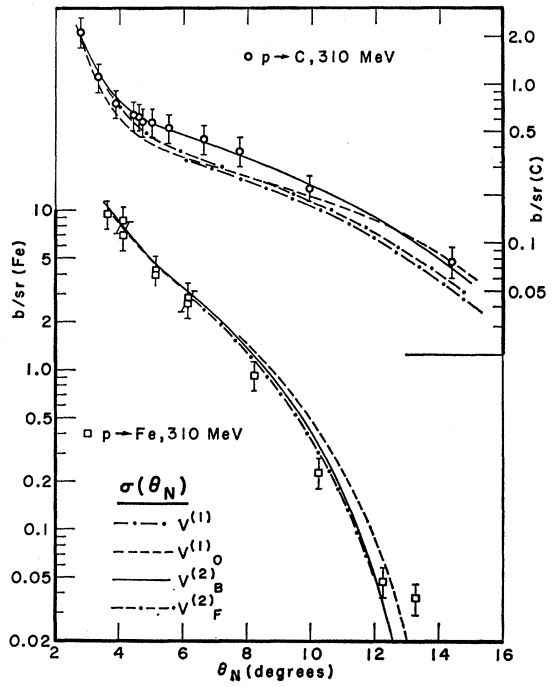

FIG. 13. Differential cross-section data for protons incident on C and Fe at 310 MeV, compared with theoretical predictions. Notation is that of Fig. 5.

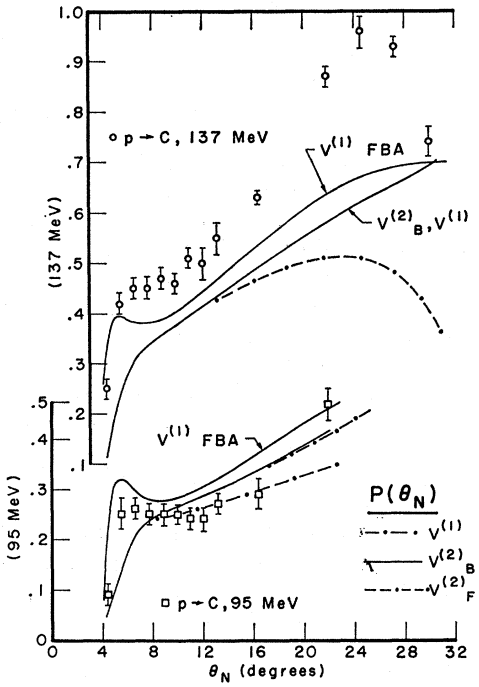

FIG. 14. Polarization data for protons incident on C at 95 and 137 MeV, compared with theoretical predictions. Notation is that of Fig. 5. The curves labeled FBA result from using the first Born approximation for the potential $V^{(1)}$. In this figure the curve $V_0^{(1)}$ is indistinguishable from $V^{(1)}$.

Comparisons with data in Figs. 14–16 show a major discrepancy: although the small-angle polarization is consistent throughout, at lower energies the theoretical polarization does not reach the experimental maximum, while at higher energies the maximum theoretical values are too large by about the same amount. The recent work of Jarvis and Rose,[40] which shows that the polarization results of Dickson and Salter[38] presented in Fig. 14 should be reduced by 15%, causes a decrease in the discrepancy at 137 MeV for p-C polarization, but does not remove it.

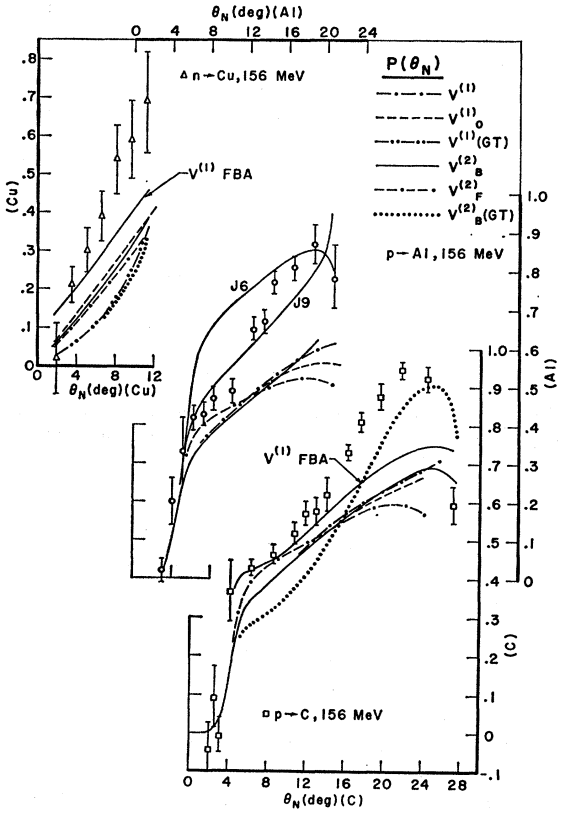

FIG. 15. Polarization data for protons incident on C and Al at 156 MeV, and for neutrons incident on Cu at 156 MeV, compared with theoretical predictions. Notation is that of Figs. 5 and 14. The curves *J*6 and *J*9 correspond to phenomenological results of Johansson *et al.* (Ref. 33). Compare also the potentials in Figs. 2–4.

The theoretical results for polarization are found to be quite insensitive to the several refinements in the calculated potential discussed in this work, as might be expected from the fact that a ratio of scattering amplitudes is involved so that changes in magnitude of the amplitudes tend to cancel out. For example, the curve marked $V^{(1)}$(BA) in Fig. 15 is the result of using the first Born approximation for the nucleon-nucleus scattering amplitude from the potential $V^{(1)}$ added to the exact Coulomb amplitude. The agreement with the exact calculation with $V^{(1)}$ is good, although the Kohler-Levintov[9] theorem does not strictly apply since the

[40] O. N. Jarvis and B. Rose, Phys. Letters **15**, 271 (1965).

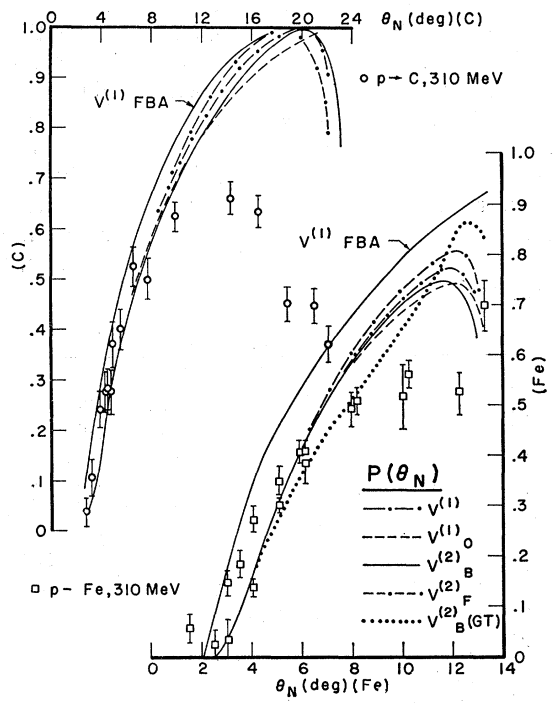

FIG. 16. Polarization data for protons incident on C and Fe at 310 MeV, compared with theoretical predictions. Notation is that of Figs. 5 and 14.

radial dependence of $V_s^{(1)}$ is not proportional to the radial derivative of $V_c^{(1)}$, and the proof of the theorem fails when two potentials are present. The discrepancy between theoretical and experimental polarization noted is not, therefore, reduced significantly by the successive approximations to the nucleon-nucleus potential studied here.

An exception to the several illustrations of the discrepancy is the curve corresponding to use of the GT phase-parameters at 156 MeV (Fig. 15) for the polarization of protons on carbon. In this case the theoretical peak value and shape are more nearly consistent with experiment than other examples. This confirms the calculation of Johansson *et al.*[35] made in first Born approximation. However, this fit must be regarded as accidental, as a study of all the GT cases in Figs. 5, 15, and 16 will show. For example, the theoretical proton-iron polarization at 310 MeV (Fig. 16) shows a discrepancy of the same type as observed with the Yale phase parameters.

The discrepancy in fit to the polarization data has also been noted at 310 MeV by Cromer[16] and Batty,[41] but in the absence of results from other energies and a variety of targets they suggested an explanation based on the experimental uncertainty in separating effects of inelastic scattering. It appears from this work that a theoretical explanation must first be sought.

[41] C. J. Batty, Nucl. Phys. **23**, 562 (1961).

There is a slight A dependence of the discrepancy: it is a little smaller for heavier nuclei than for light, but there are not enough examples at enough energies to make this point strongly. It appears particularly important to have more polarization data available, especially in the 150–350-MeV range of energies and also at lower energies for incident neutrons to illuminate this disagreement between theory and experiment.

The phenomenological potentials predict a polarization maximum in general agreement with the data (see Fig. 15) and it has long been known that this is possible over a range of energies and targets.[42] One may see the principal source of difference between the phenomenological and theoretical polarization predictions in Fig. 1. Here the phenomenological value of VSI is considerably larger than the theoretical curve at 160 MeV, and smaller at 300 MeV. As Figs. 15 and 16 show, this is just the correction needed for the theoretical potential. While there is more in detail to it than this, most of the discrepancy between theory and experiment can be made up by the indicated changes in VSI. It will be seen in Sec. IV that no immediate modifications of the theory are likely to produce the variations with energy of VSI as shown for the phenomenological cases in Fig. 1.

IV. ESTIMATES OF EFFECT OF APPROXIMATIONS AND PARAMETER VARIATIONS

A. The Impulse Approximation

The error incurred by replacing $\mathbf{t}_\alpha$ in Eq. (3) by the free nucleon-nucleon operator t_α has been estimated by Fowler and Watson[43] to be of order $(B_{\rm av}/2\epsilon_0)f/\lambda$, where $B_{\rm av}$ is the average binding energy of nucleons in the nucleus, f is the scattering amplitude. This predicts an error of about 10% at 100 MeV and 5% at 300 MeV. If the propagator for t is corrected by including the dispersive energy of the nucleon moving in the nuclear medium,[44] the relative error is reduced to $(B_{\rm av}^2/8\epsilon_0^2)f/\lambda$; i.e., about 1% and 0.5%, respectively, at 100 and 300 MeV. A numerical estimate of this correction may be made by evaluating the two-nucleon t matrix at an energy lower than the experimental energy. Calculations were made with energy shifts of 18 MeV and 35 MeV, respectively, for an incident energy of 95 MeV, and 19 and 28 MeV for an incident energy of 156 MeV. The cross-section predictions are raised several percent by these shifts, in general agreement with the Fowler-Watson estimate, so that the error due to the impulse approximation, quite roughly estimated here, may be of the order at low energies of the corrections to $V_0^{(1)}$

[42] F. Bjorklund, I. Blandford, and S. Fernbach, Phys. Rev. **108**, 795 (1957); F. Bjorklund and S. Fernbach, in *Proceedings of the Second International Conference on Peaceful Uses of Atomic Energy*, (United Nations, Geneva ,1958) Vol. 14, p. 24.

[43] T. K. Fowler and K. M. Watson, Nucl. Phys. **13**, 549 (1959); see M. L. Goldberger and K. M. Watson, *Collision Theory* (John Wiley & Sons, Inc., New York, 1964) for a detailed account.

[44] K. M. Watson, Phys. Rev. **105**, 1388 (1957).

given by the integrated potential and the second-order contributions. The polarization predictions are hardly affected by the estimated changes, and the discrepancy in cross-section level at higher energies for heavy nuclei is not removed.

B. Neglect of Target-Nucleon Momentum

Momenta of the target nucleons may be 35% of that of the incident nucleon, but being isotropically distributed it is expected that in taking the average of the t matrix their momenta may be taken as zero. A numerical estimate,[29] drawing on work of Dabrowski *et al.*,[45] shows that for incident energies above 100 MeV a change in $\mathrm{Im}V^{(1)}$ of less than 3% results from assuming zero target momentum.

C. On-Energy-Shell Approximation

The error in using free-nucleon kinematics has been estimated by evaluating the factors relating the t matrix in the nucleon barycentric system to that in the nucleon-nucleus system, assuming nucleon-nucleus kinematics.[46] The correction factor is unity at forward angles and decreases to 0.63 at the maximum momentum transfer allowed by the free nucleon kinematics. However, in the integrated potentials, the principal contributions to $V^{(1)}$ are from forward angles, so the effect on the potentials is small.

A rough estimate of the effect of evaluating the two-nucleon scattering matrix off the energy shell was obtained by using the first Born approximation for scattering amplitudes calculated from the nucleon-nucleon potentials fitting the scattering data.[47] This calculation was used to continue t off the energy shell: the magnitude was fixed by making it agree with the phase-parameter results on the energy shell. Only the central and spin-orbit parts of the potential contribute to $A(\theta)$ and $C(\theta)$ of Eq. (7), and only $C(\theta)$ is affected in these estimates. The correction obtained for ranges of q required by the nucleon-nucleus kinematics produces a change of about 5% in the polarization for high energies and heavy targets and less otherwise, and this is much too small to remove the discrepancies in the fit to polarization already noted.

D. Antisymmetrization Approximation

The failure to antisymmetrize the wave function for $A+1$ nucleons neglects target exchange, as has been mentioned. Takeda and Watson[22] estimate that correct antisymmetrization would introduce a correction of order 3% at 100-MeV incident energy, and a smaller one at higher energies. In a more recent calculation, Sawicki[48] develops a correction for the optical potential which includes target exchange terms. These corrections are of order 0.5% at 80 MeV and 0.1% at 230 MeV, and thus are smaller than others discussed above.

E. Variation of Nuclear-Structure Parameters

Although the assumption that the charge and nucleon distributions are the same, and that electron-scattering analysis gives the charge distribution, does not allow the parameters of $\rho(r)$ to be considered free in this calculation, the effect of variations has been investigated. It was found that at 300 MeV (Fig. 6) an increase of 10% in the range parameter produced a further "rotation" of the theoretical curve for $\sigma(\theta)$, which tends to improve the angular dependence in comparison with experiment. Excellent agreement with the data could be then achieved by increasing the magnitude of the Brueckner-Gammel-type correlation lengths to $R_s=R_a=-2.10$ F, an increase by a factor 2.5. Similar results were obtained by increasing the surface parameter by 30% and the correlation lengths by a factor 2.75. The polarization prediction is reduced by these changes, but by only about one-tenth the amount necessary to produce agreement with experiment. At higher energies these changes would produce similar improvements in all cases, but at lower energies only the increases in range and surface parameters would be allowed by the data. The polarization discrepancy would, in any case, remain. While these calculations suggest that the nucleon distribution might be longer ranged than the charge distribution, and that the correlation lengths should be larger in magnitude than those given by the Brueckner-Gammel wave functions, there is not complete consistency for all data at all energies. In view of the uncertainties in the theoretical calculations, outlined above, such conclusions are not justified. For example, better treatment of off-energy-shell behavior of the t matrix might give greater extent to the nuclear potential with use of the original shape parameters for the matter distribution.

F. Variation of Nucleon-Nucleon Phase Parameters

Recent improvements[20] in the phase-parameter fits to nucleon-nucleon data have also been considered in these calculations. The differences between these and the older fits[12,18] used in the bulk of the calculations is much smaller than between the Gammel-Thaler parameters and the older fits, and the changes in nucleon-nucleus cross-section and polarization curves are at most 4%, which is well within both experimental and theoretical uncertainties. An arbitrary change of the magnitude of $C(\theta)$ to produce agreement with nucleon-nucleus polarization is completely incompatible with nucleon-nucleon data.

---

[45] J. Dabrowski and J. Sawicki, Ref. 14.
[46] C. Møller, Kgl. Danske Videnskab. Selskab, Mat. Fys. Medd. **23**, 1 (1945).
[47] K. Lassila, M. H. Hull, Jr., H. Ruppel, F. A. McDonald, and G. Breit, Phys. Rev. **126**, 881 (1962).
[48] J. Sawicki, Nuovo Cimento **15**, 606 (1960).

V. SUMMARY AND CONCLUSIONS

In common with earlier work[10–14] the first-order nucleon-nucleus potential with nucleon distribution given by electron scattering reproduces the experimental cross section in order of magnitude when the newer phase parameter analyses are used for the two-nucleon scattering matrix. Use of the integrated potentials, including angular dependence of the nucleon-nucleon scattering matrix,[16] improves the angular dependence of the cross section, and addition of the second-order potential[15] with Brueckner-Gammel correlation lengths generally improves agreement with data in magnitude. These two corrections are of the same order of magnitude, and must both be included on the same footing in a consistent calculation. At higher energies and for heavier targets, the improvements do not succeed in producing a good fit to the cross-section data, however.

The polarization predictions are relatively insensitive to the corrections discussed, and the theoretical potentials do not lead to a fit to the experimental values near the first maximum, although at lower angles there is general agreement with data. This disagreement is emphasized by use of the more recent[17,18] nucleon-nucleon phase parameters. The importance of comparing predictions with data over a range of energies and targets is brought out in detailing this discrepancy, and the desirability of further experiments for neutron polarization at all energies and proton polarization between 200 and 300 MeV for several targets is indicated.

Estimates of the errors in the theoretical treatment do not suggest an answer to the polarization discrepancy, since all the estimates indicate effects much too small, and none clearly has the needed energy dependence. At the same time, the estimates are large enough to suggest caution in drawing conclusions about nuclear-structure parameters and in attempting to select from among several good fits to nucleon-nucleon data by an analysis along these lines of nucleon-nucleus scattering.

However, the generally good agreement between the present calculation and a wide range of data as illustrated in Figs. 5–16 should not be overlooked. No *ad hoc* parameters have been introduced: the phase shifts come from analyses of nucleon-nucleon scattering, the nuclear charge distribution parameters from electron-nucleus scattering, and the correlation lengths from models of the nucleus used to discuss its static properties. While careful calculations, going well beyond first Born approximation estimates, have been required, rather strong evidence for the usefulness of the impulse approximation in relating nucleon-nucleon to nucleon-nucleus scattering has resulted.

Effects of third-order terms in the multiple-scattering expansion have not been estimated. The possibility that unusual contributions to the second-order term, such as strongly excited low-lying collective modes,[49] could change the potential in the required way has not been investigated. The work of Clegg[50] which appeared as the present paper was in preparation, gives some information on this point. He makes a similar suggestion to explain the same discrepancy in the polarization prediction for 155-MeV protons scattered from C^{12} found in this work. Estimating the effect on the calculated polarization of excitation followed by de-excitation of states in the target nucleus of a specific type such as are identified experimentally, he makes it plausible that an enhancement of the predicted polarization values is possible. However, no calculations are given, and the question of the *reduction* in predicted polarization required at higher energies is not investigated.

ACKNOWLEDGMENTS

The authors would like to thank the Yale nucleon-nucleon group, headed by Professor G. Breit, and including Dr. H. M. Ruppel, Dr. A. N. Christakis, and R. E. Seamon, for providing phase-parameter sets in convenient form for use in the present calculation. The authors also wish to thank Professor Breit for calling their attention to the work of Jarvis and Rose.

[49] One of the authors (MHH) would like to thank Dr. Carl M. Shakin for a conversation on this point.
[50] A. B. Clegg, Nucl. Phys. **66**, 185 (1965).